Cerebral Cortex, February 2017;27: 1103–1112

doi:10.1093/cercor/bhv299
Advance Access Publication Date: 9 December 2015
Original Article

ORIGINAL ARTICLE

Spatially Tuned Neurons in Corvid Nidopallium Caudolaterale Signal Target Position During Visual Search

Lena Veit, Konstantin Hartmann and Andreas Nieder

Animal Physiology, Institute of Neurobiology, University of Tübingen, 72076 Tübingen, Germany

Address correspondence to Andreas Nieder, Animal Physiology, Institute of Neurobiology, Auf der Morgenstelle 28, University of Tübingen, 72076 Tübingen, Germany. Email: andreas.nieder@uni-tuebingen.de

Abstract

The avian pallial endbrain area nidopallium caudolaterale (NCL) shows important similarities to mammalian prefrontal cortex in connectivity, dopamine neurochemistry, and function. Neuronal processing in NCL has been studied with respect to sensory, cognitive, and reward information, but little is known about its role in more direct control of motor behavior. We investigated NCL activity during the choice period of a delayed match-to-sample task, as 2 trained crows searched and selected a previously remembered visual target among an array of 4 pictures. The crows exhibited behavioral response patterns consistent with serial visual search. Many single NCL neurons were spatially tuned to specific target positions during visual search and directed motor behavior. Moreover, single NCL neurons dynamically changed their tuning properties to represent different behaviorally relevant task variables across the trial. In consecutive task periods, single neurons responded to visual stimuli, stored stimulus information in working memory, guided goal-directed behavior depending on the remembered target picture, and encoded trial outcomes. This flexible encoding of all task-relevant aspects in the executive control of goal-directed behavior represents a striking convergence to neuronal encoding in primate prefrontal cortex. These data highlight key properties of associative endbrain areas underlying flexible cognitive behavior in corvids and primates.

Key words: crow, executive control, pallial evolution, prefrontal cortex, single-unit recording

Introduction

Corvid birds such as crows exhibit remarkable cognitive abilities (Clayton and Emery 2015) and can perform precise directed actions to specific locations in space, for example during tool use (Taylor et al. 2009), spatial memory tasks (Clayton and Dickinson 1998; Emery and Clayton 2004), and rule-guided choices (Moll and Nieder 2014). The multimodal cognitive association area nidopallium caudolaterale (NCL) is emerging as a key brain structure for executive control of behavior in birds (Güntürkün 2005). Like the independently evolved prefrontal cortex of mammals (Miller and Cohen 2001; Fuster 2008), NCL lies at the intersection of sensory, motor, and reward systems and is thought to integrate these various types of information in the control of goal-directed behavior (Güntürkün 2005). Similar to prefrontal neurons in monkeys, single neurons in NCL signal the number of visual stimuli (Ditz and Nieder 2015), working memory (Veit et al. 2014), abstract behavioral rules (Veit and Nieder 2013), learned associations (Moll and Nieder 2015; Veit et al. 2015), expectation of reward, and behavioral outcomes (Kalenscher et al. 2005; Starosta et al. 2013). By comparing neuronal processing in independently evolved associative endbrain areas, we hope to reveal general principles and evolutionary constraints underlying neuronal processing of executive function in highly cognitive vertebrates.

In addition to encoding cognitive aspects of behavior, NCL might play a more direct role in motor behavior during the execution of movement following cognitive processing. Anatomically, NCL receives input from sensory association areas and is connected to (pre-)motor areas of the arcopallium (Kröner and Güntürkün 1999). NCL also receives dopaminergic projections

from midbrain dopamine centers and has strong connections to sensorimotor striatum (Wynne and Güntürkün 1995; Durstewitz et al. 1999). Therefore, in addition to integrating sensory information and processing it with respect to internal goals and reward, NCL is well positioned to ultimately also exert influence on motor actions.

To explore processing patterns of single NCL neurons during visual search behavior, we analyzed neuronal activity during the choice period of a delayed match-to-sample (DMS) task. The task required the crows to remember a briefly presented sample picture, to hold it in working memory over a delay period, and finally to find it again among 4 different pictures in order to receive a reward. We recorded single neurons in trained carrion crows as they searched and selected the previously remembered picture in a choice array of 4 complex visual pictures on a touchscreen. We find that single NCL neurons were strongly activated by specific target positions during this period of visual search and visually guided directed motor behavior.

Materials and Methods

Subjects

Two female carrion crows (*Corvus corone corone*) were used in these experiments. For details on the birds' housing and diet, see Hoffmann et al. (2011). The crows were obtained from the institute's breeding facilities, hand-raised, and trained on a DMS task. The crows were maintained on a controlled feeding protocol during the sessions and earned food during and after the daily tests. All procedures were carried out according to the guidelines for animal experimentation and approved by the responsible national authorities, the Regierungspräsidium Tübingen, Germany.

Behavioral Protocol

The CORTEX program (National Institute of Mental Health) was used for experimental control and behavioral data acquisition. The crows were positioned in front of a touchscreen monitor (3 M Microtouch, 15″, 60 Hz refresh rate). A sample stimulus was presented in the center of the screen for 500 ms. Next, a 1000-ms delay period followed, during which the crow had to remember the sample stimulus. In the choice period, 4 pictures (2 × 2 cm) appeared in 4 corners of the screen, spaced 6.6 cm apart. The set of 4 pictures was exchanged every day but remained constant within a recording session. Each of the 4 pictures was used as a sample picture on randomly alternating trials, and all 4 pictures were always presented in the choice period, with randomized and balanced position in the 4 corners of the screen. While the crows had to keep their heads in an infrared light barrier during the sample and delay periods, the head could be freely moved during the choice period. For details of the behavioral protocol, see Veit et al. (2014).

The crow indicated its choice by pecking at one of the stimuli. Following a peck, the crows received a 300-ms visual and auditory feedback if the trial was correct or not. On correct trials, reward was delivered following an additional 500-ms waiting period. During reward delivery, a custom automated feeder presented visual and auditory reinforcement, and in approximately 50% of correct trials the crow could retrieve a food reward. On error trials, the feeder did not deliver reward and a short timeout (3000 ms) was introduced before the next trial. If no response occurred within 1800 ms in the choice period, the trial was dismissed.

Surgery and Recordings

All surgeries were performed under sterile conditions while the animals were under general anesthesia. The head was placed in the stereotaxic holder that was customized for crows with the anterior fixation point (i.e., beak bar position) 45° below the horizontal axis of the instrument (Karten and Hodos 1967). Using stereotaxic coordinates (center of craniotomy: anterior-posterior 5 mm; medial-lateral 13 mm) to target the NCL, we chronically implanted 2 microdrives with 4 electrodes each. We implanted the 8 electrodes in the left hemisphere in crow I, and in both hemispheres (consecutively) in crow K. We used glass-coated tungsten microelectrodes with 2 MΩ impedance (Alpha Omega Ltd, Israel). The crows received postoperative analgesics.

At the start of each recording session, the electrodes were advanced manually until a good neuronal signal was detected on at least one of the channels of each microdrive. Signal amplification, filtering, and digitizing of spike waveforms were accomplished using the Plexon system (Dallas, TX, USA). Spike sorting into single-unit waveforms was performed offline using the Plexon system.

Data Analysis

All analyses were performed in Matlab. We analyzed behavior from all recording days on which at least one analyzed neuron was recorded ($N = 61$ days in crow K and $N = 36$ days in crow I). Reaction times (RTs) are the times from onset of the choice array until the crows' peck at one of the test images.

The analysis includes all neurons which were recorded for at least 2 repetitions of each target picture and target position and had a firing rate of at least 0.5 Hz in a 1-s window after choice onset. Only correct trials are included in the analyses. We recorded a total of 184 neurons in crow K and 176 neurons in crow I ($N = 360$). We used a two-factor ANOVA to determine whether each neuron's discharge rates differed significantly for the 4 different target pictures or target positions ($P < 0.05$).

To control for nonspecific motor activity without position-selectivity, we sorted the trials for each target position by their RTs and performed a ranksum test between the firing rates in the first and third quartile of trials for each position (Fig. 3*D*). We did not select the fourth quartile for this analysis because RTs were most variable during this quartile. If any of these 4 tests gave a significant result ($P < 0.05$), the neuron's firing rate was considered to be influenced by the crow's RT and excluded from analyses of pure position-tuning.

For neurons that encoded target positions and were not influenced by RT, we calculated normalized tuning curves by scaling each neuron's firing rates between 0 and 1, and then averaging across neurons with the same positional tuning preference. Additionally, we used a selectivity index to quantify the strength of tuning to individual positions (Miller et al. 1996; Vallentin and Nieder 2010; Veit et al. 2014):

$$\mathrm{ST} = (\mathrm{FR\_max} - \mathrm{FR\_min})/(\mathrm{FR\_max} + \mathrm{FR\_min}),$$

where FR_max is the cell's discharge rate to the preferred target position and FR_min is the firing rate to the least preferred target position, that is, the one that elicited the lowest discharge rate. Thus, selectivity strength is a value between 0 and 1, with values close to 1 indicating very strong selectivity.

To better quantify the degree by which individual neurons were influenced by target position, target picture, and RTs, we performed a multiple linear regression of each neuron's firing

rate onto regressors for target position, target picture, and RT (Fig. 3E). For each neuron, we modeled the firing rate in each trial as a linear weighted sum of predictors depending on the trial type. Each neuron's firing rates in all trials form a vector y with as many elements as trials for this neuron. Similarly, the type of trial is translated into a series of vectors of the same size, which encode the position, picture, and RTs. We used contrast coding for categorical predictors, that is, target picture and target position, so that the possible values for these predictors are encoded by a series of binary vectors. Since there were 4 possible positions, we needed 3 binary vectors in order to encode all possible combinations of position preferences. One of these vectors, for example, would contain a 1 for target positions on the left, and a –1 for target positions on the right. The next regressor would encode the top versus bottom position, and the third an interaction between top and bottom, that is, preference for top left and bottom right, versus, top right and bottom left. Similarly, there were 3 binary vectors to encode the 4 possible target pictures, and 1 numerical vector of RTs. Next, we estimated the weights for the individual predictor vectors using the equation:

$$y = \beta_0 + \beta_1 * x_1 + \beta_2 * x_2 + \ldots + \beta_7 * x_7 + \varepsilon,$$

where β_0 is a constant, independent of trial type, and ε is an error term. Therefore, for each neuron, there are 7 regression coefficients β_1 to β_7, indicating the weight that each trial type variable has for determining this neuron's firing rate. To estimate the beta-values, we performed generalized linear model regression using the MATLAB statistics toolbox.

To compare the encoding of different task variables across task periods, we performed a sliding analysis of ω^2, which is a measure of effect size that reflects how much of a neuron's firing rate can be explained by each task variable. We calculated ω^2 separately for the 3 factors sample picture, target position, and trial outcome, for each neuron using the equation:

$$\omega^2 = (SS_{effect} - DF * MS_{error})/(SS_{total} + MS_{error}),$$

where SS_{effect} is the sum of squares between groups, SS_{total} is the overall sum of squares, DF is the degrees of freedom, and MS_{error} is the mean squared error within groups (Hentschke and Stüttgen 2011). The analysis was performed in a 300-ms sliding window advanced in steps of 20 ms across the entire trial, aligned both by sample onset (Fig. 6E) and by the crow's response (Fig. 6F).

Additionally, each neuron's selectivity was evaluated in different windows of interest using statistical tests. Sample selectivity was evaluated in a 500-ms window starting 80 ms after sample onset (sample period), and an 800-ms window starting 200 ms after sample offset (delay period) using a Kruskal–Wallis one-factor ANOVA, as in Veit et al. (2014). Choice period selectivity was evaluated using a two-factor ANOVA with factors target picture and target position in a 300-ms window starting 350 ms before the crow's response. Selectivity for trial outcome was evaluated in a 500-ms window starting 200 ms after reward delivery using a ranksum test between correct and error trials.

Results

Visual Search Behavior

We analyzed the choice period of a delayed matching-to-sample task, in which crows had to search and select a previously remembered stimulus from an array of 4 test images on a touchscreen (Fig. 1). The 4 test images were exchanged daily but kept constant during 1 recording session. Each test item's position on the screen was randomized and balanced among the 4 possible positions. The correct target was therefore distributed equally in all 4 corners of the screen.

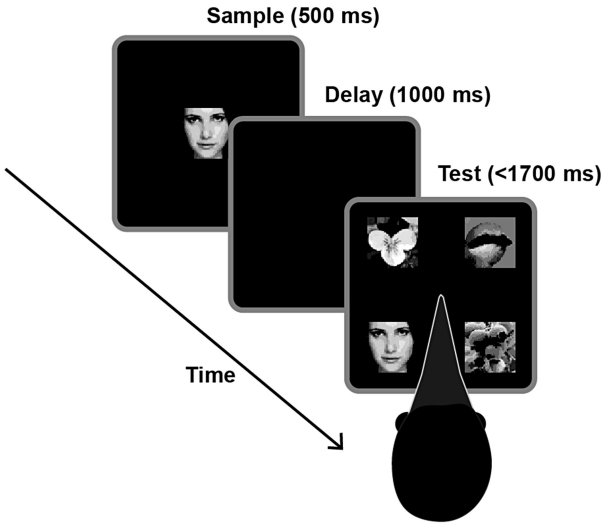

Figure 1. DMS protocol. The crow was presented 1 of 4 pictures in the center of the screen. After a brief memory delay (1 s), the crow had to select the previously seen image from an array of 4 images shown during the test phase. The position of the target image and the 3 distractor images were randomized and balanced.

The crows displayed differences in behavioral performance and RTs for the 4 different positions. For both crows, performance for individual target positions was significantly different (both $P < 0.001$, Friedman test), but was clearly above chance for all positions (Fig. 2A,B). RTs also differed among target positions in both crows (both $P < 0.01$, Friedman test; Fig. 2C,D). When ordering positions by decreasing performance, or increasing RTs, the same order of target positions emerged for each crow indicating a consistent search pattern to scan the choice screen (Fig. 2E,F). On average, crow K started its search at the "bottom right" position, moved to the "bottom left", then switched up to the "top right" and finished at the "top left" position. Crow I showed an alternative scan path by moving from the "left bottom" position in a counter-clockwise direction from "bottom right" to "top right" and finally the "top left" position.

Neuronal Selectivity for Target Position

We analyzed the activity of 360 neurons during the response period. To determine how single NCL neurons encoded target position during the choice period, we performed a two-factor ANOVA with factors target picture and target position on firing rates in a 300-ms window from 350 ms before response to 50 ms before response. The shortest RT in any trial was 383 ms, so that this window always lay entirely within the response phase.

Figure 3A,B shows an example neuron selective for target position. The discharges of the neuron as a function of target position are aligned relative to test items onset (Fig. 3A) or relative to the crow's response (Fig. 3B). This neuron discharged vigorously for responses on the right side of the screen (green and blue colors, respectively, in the spike density histograms in Fig. 3A,B), and briefly suppressed activity during responses on the left side of the screen (Fig. 3B). This neuron showed a significant main effect of target position but no significant effect of target picture, and no interaction ($P < 0.001$ and $P = 0.16$, respectively; two-factor ANOVA; Fig. 3C).

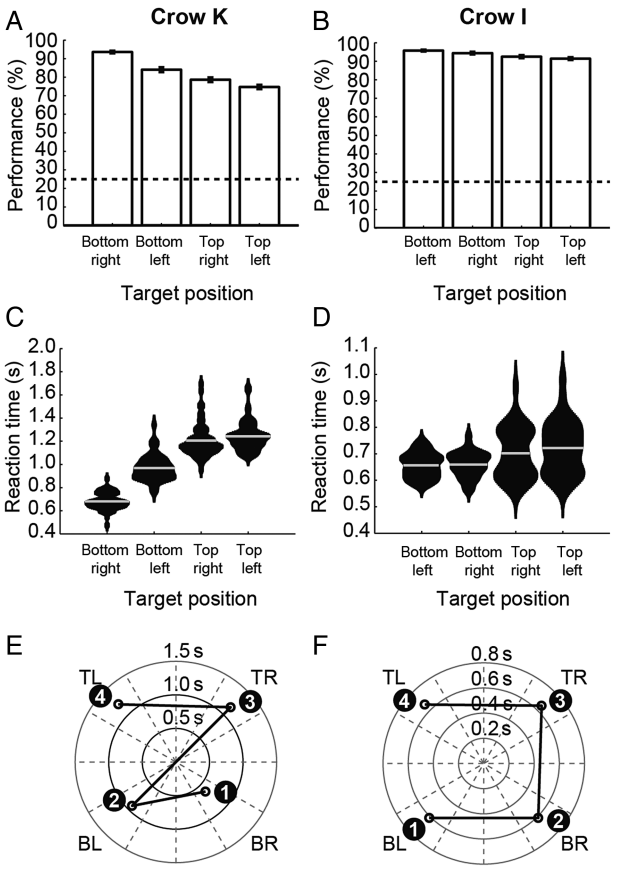

Figure 2. Visual search behavior. (*A* and *B*) Behavioral performance for each target position, with target positions ordered by decreasing performance. Error bars indicate SEM across days ($N = 61$ days crow K, $N = 36$ days crow I). Dotted line indicates chance level 25%. (*C* and *D*) Violin plot of RTs for each target position for each recording day smoothed using a Gaussian kernel. White line indicates mean over recording days. Target positions are ordered by increasing RTs. (*E* and *F*) Sketch of search pattern for crow K and crow I, as found in performance and RTs, plotting mean RTs for each target position. Black circles indicate a serial order of target in the bird's search pattern.

As the crows' behavioral response times systematically varied for different target positions (Fig. 2*C*,*D*), it is possible to get false-positive results for the position factor in the ANOVA by response-related neuronal activity that is not tuned to target position. For instance, comparing the same nonselective ramping activity in different time windows might result in artificial firing rate differences. To control for this aspect, we performed a ranksum test between the firing rates in the first and third quartile of all trials for each target position ordered by their RTs, that is, between the fastest quarter of trials for each target position and a slower quarter of trials. The example neuron in Figure 3 did not show significant differences between fast and slow trials for any target position ($P > 0.05$ ranksum test, Fig. 3*D*).

Qualitatively similar results are obtained by a multiple linear regression on target position, sample picture, and RT (see Materials and Methods). The example neuron showed a large significant beta-weight for left/right position, and a small significant beta-weight for top/bottom position, with no other regressor significantly influencing the neurons' firing rates (Fig. 3*E*). These regression weights reflect the neuron's preference for bottom right positions. This analysis confirmed that spatial position of the target, not target identity or RT, was encoded by the neuron.

Overall, 64% of all recorded neurons (231/360) were unaffected by RT for any target position ($P < 0.05$, ranksum test). Of these neurons, 36% (83/231) had a significant main effect of target position and no interaction [$P < 0.05$, two-factor ANOVA; overall 151/360 (42%) with RT effect], and 55/231 (24%) had a significant main effect of target picture and no interaction [overall 97/360 (27%) with RT effect; Table 1].

We quantified spatial tuning of the 83 position-selective neurons showing no RT effect. Figure 4*A* shows example spatial tuning curves of 4 different neurons. The test location that elicited the highest firing rate for a neuron was called the "preferred position." The neuron in green color and preferring the bottom right position is the example neuron from Figure 3. Figure 4*B* shows normalized neuronal tuning curves of all selective neurons according to their preferred positions. The tuning to individual target positions of these selective neurons was quite sharp: Comparing each neuron's response to the preferred and least preferred position, the neurons had an average selectivity index of 0.49, corresponding to a 292% increase in discharge rate to the preferred compared with the least preferred position.

The 4 spatial quadrants might have been segregated into 2 categorically distinct spatial compartments, such as top versus bottom, or left versus right. The example neuron in Figure 3 invites this suspicion because it is most prominently influenced by the left/right position of the target. To evaluate how prevalent such tuning patterns to, for example, all positions on the left, or all positions on the top, were in position-tuned neurons, we show the entire populations' individual beta-values for the left/right position regressor and the top/bottom position regressor (Fig. 4*C*). However, there was no clear segregation into different subpopulations of spatially selective neurons. Instead, the neuron population formed a continuum of all combinations of different beta-values, that is, different tuning strengths for samples on the left or top of the screen and combinations of these.

No Hemispheric Differences in Spatial Encoding

We wondered whether the degree of left/right spatial tuning might have been a function of the recorded hemisphere. Figure 5*A* shows the distribution of preferred position for all position-selective neurons ($N = 83$) according to their recording location in the left NCL of crow I, or in the left or right NCL of crow K. The white numbers indicate the number of neurons preferring each target position, whereas the shading indicates the percentage of spatially tuned neurons preferring each position. The figure shows that neurons with all possible target preferences were recorded in each hemisphere, and each crow contributed neurons preferring each position. There was no consistent pattern of neurons in one hemisphere exhibiting stronger preferences for target locations on the ipsi- or contralateral side of the screen. Similarly, the individual regression beta-values for the ipsi- and contralateral side of the screen were not significantly different ($P = 0.75$, ranksum test, Fig. 5*B*).

Comparison of Selectivity in the Choice Period with Other Task Periods

NCL neurons are known to encode different sensory, cognitive, and motor variables. We therefore investigated the capacity of single neurons to represent different task variables. Individual neurons were tested for selectivity to sample picture in the sample and delay periods, and to trial outcome in the reward period, to compare their selectivity in different trial periods to their encoding of target picture or position in the choice period. We

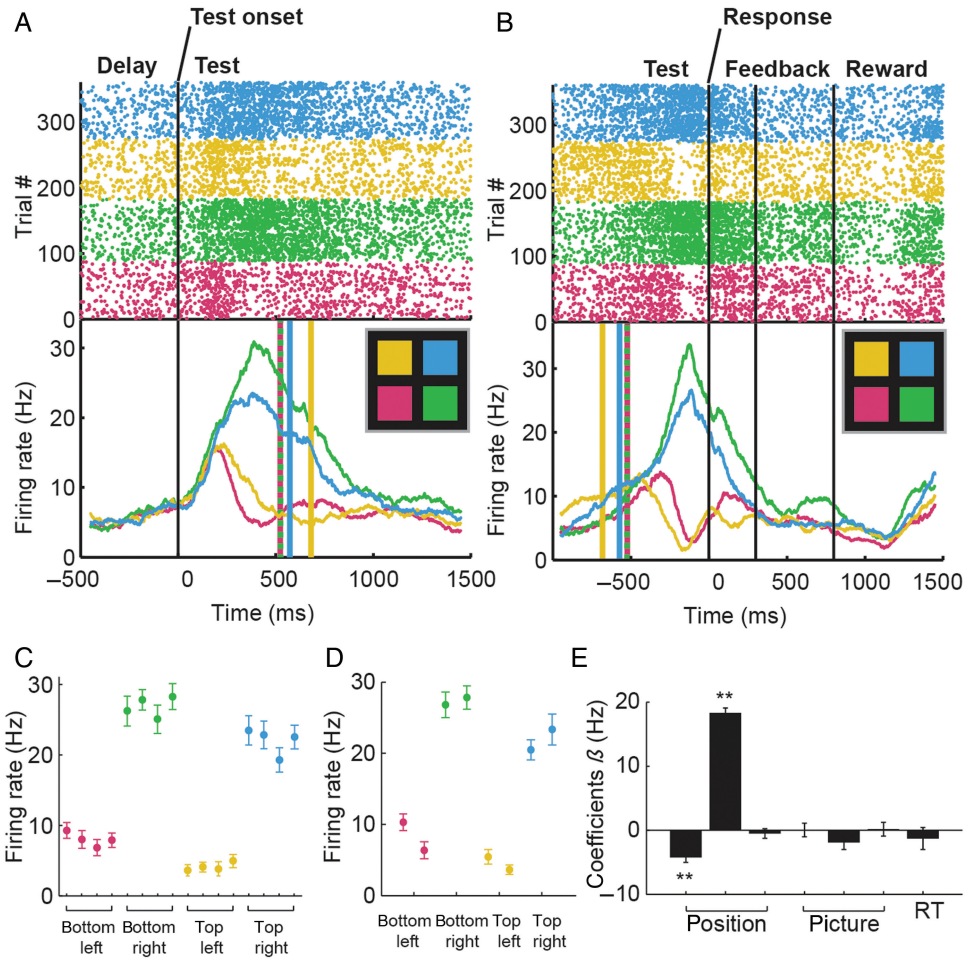

Figure 3. Example neuron selective for target position. (*A*) Responses of the neuron aligned relative to test items onset. The neuron showed higher discharge rates for target positions on the right side of the screen. (Top) Dot-raster histogram; each dot represents an action potential; colors indicate different target positions. Trials are ordered by target position, and actual presentation order was randomized. (Bottom) Peri-stimulus time histogram obtained by averaging the dot raster across trials of one condition and smoothing with a 150-ms boxcar window. Vertical black line indicates test period onset, and vertical colored lines indicate median response times for the different target positions. (*B*) Same neuron as in *A*, but discharges aligned relative to the crow's response (time = 0 ms). Vertical colored lines indicate median choice onset times for different target positions. (*C*) Firing rates in response to the 4 different target pictures in each of the 4 target locations. Only target position, but not target identity, modulated the discharge rates. Error bars indicate standard error of the mean (SEM). (*D*) Firing rate in response to the 4 different target locations in the fastest quartile of trials and the third fastest quartile of trials for each target location. This neuron's firing rate was unaffected by RTs in any of the 4 target locations. Error bars indicate SEM. (*E*) Regression weights for a multiple linear regression on 3 regressors for the 4 target positions, 3 regressors for the target picture, and RTs. This neuron's firing rate was significantly affected by the top/bottom (first-position regressor) and left/right (second-position regressor) position of the target, and not significantly influenced by any other explanatory variable. Error bars indicate SEM.

Table 1 Selectivity in the choice period

Percentage of cells selective for	All neurons ($N = 360$)	Neurons without RT effect ($N = 231$)
Target position	42% (151/360)	36% (83/231)
Target picture	27% (97/360)	24% (55/231)
Both picture and position, no interaction	17% (61/360	12% (28/231)
Interaction between picture and position	23% (82/360)	20% (46/231)

Note: Number of cells selective for different factors according to a two-factor ANOVA (target position × target picture) in a 300-ms choice period window ending 50 ms before the crow's response. The numbers for target picture and position include the neurons which are selective for both factors.

found that 89% of all neurons participated in selective encoding of task events during any task period. Table 2 summarizes the different types of selectivity encountered. Interestingly, only 50% of neurons, which were selective to the identity of the target picture in the response period, exhibited sample selectivity in the sample period.

Furthermore, a large fraction of neurons, which were selective for target position in the test period, previously exhibited selectivity for the sample picture in the sample or delay periods. This indicates that individual neurons can dynamically change their tuning properties throughout the trial to represent different behaviorally relevant types of information. Figure 6*A–D* shows an individual example neuron, which was selective for sample picture in the sample and delay periods (both $P < 0.01$, Kruskal–Wallis one-factor ANOVA). In the choice period, this neuron was responding selectively for the same 2 samples ($P < 0.001$, two-factor ANOVA), in addition to position-selectivity for targets in the top half of the screen ($P < 0.05$, two-factor ANOVA), but no interaction ($P = 0.27$, two-factor ANOVA). Finally, this neuron significantly discriminated correct and error trials during the reward period ($P < 0.05$, ranksum test).

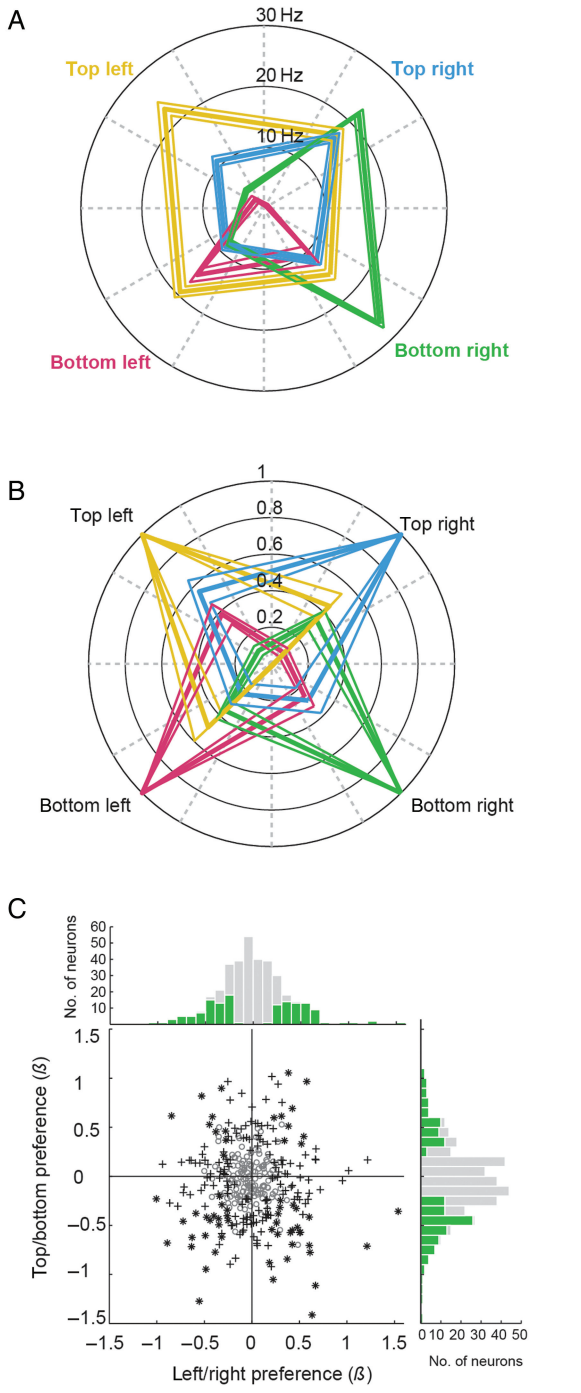

Figure 4. Spatial tuning curves. (*A*) Mean tuning curves of 4 position-selective units, one for each preferred position. The colors indicate preferred position. The green neuron is the example neuron from Figure 3. Thin lines show SEM across trials. (*B*) Mean tuning curves of all position-selective units that did not show an influence by RT. Each neuron's firing rate was normalized between 0 and 1 before averaging tuning curves of different neurons with the same position preference. Thick lines show mean firing rate for the 4 different positions, and thin lines show SEM across neurons. Colors indicate preferred position. (*C*) Center: Regression weights (beta-values) obtained by a multiple linear regression analysis for the top/bottom and left/right regressor of target position. Each dot represents one neuron. Shading represents significance. Gray circles: neither top/bottom, nor left/right, preference was significant. Black cross: one of the top/bottom or left/right preference was significant. Black star: both top/bottom and left/right preference were significant. Top and right: Histograms of beta-weights for the top/bottom and left/right regressor, with significant weights colored green.

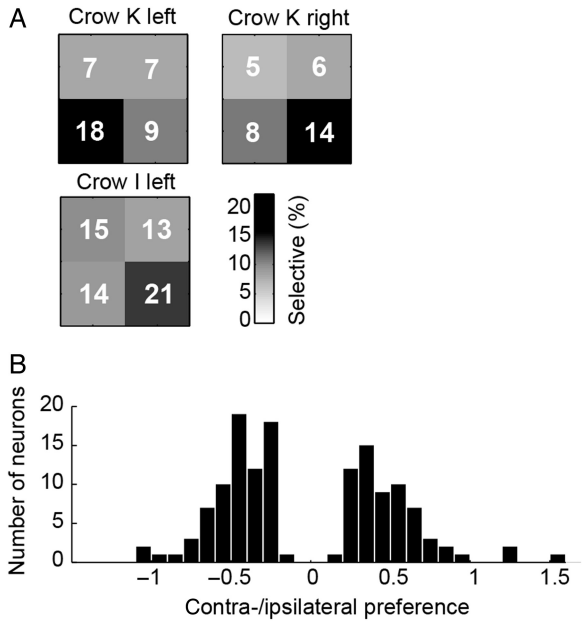

Figure 5. Anatomical distribution of spatial preferences. (*A*) Number (white numbers) and percentage (shading) of spatially tuned neurons preferring each target position recorded in each hemisphere. (*B*) Regression weights (beta-values) obtained by a multiple linear regression analysis for the left/right regressor ordered by their recording location, indicating preference for contra- or ipsilateral target positions.

To quantify what aspects of the task (target picture, target position, and trial outcome) were influencing neuronal activity at different time points in the trial, we performed a sliding analysis of explained variance by these different task variables (Fig. 6*E*,*F*). In the first parts of each trial (sample and delay periods), the target picture (i.e., sample picture) is the only variable which is known to the crow and the only one of the analyzed variables influencing neuronal activity. Sample selectivity during the sample and delay periods and its role in visual working memory has been previously discussed (Veit et al. 2014). After test onset (Fig. 6*E*), the target picture is initially the strongest factor influencing neuronal selectivity, as in the preceding sample and delay periods. Selectivity by target position starts to appear approximately 200 ms after test onset, and quickly becomes the strongest information represented in the recorded population (Fig. 6*E*).

Similar results appear if the same neuronal activity as in Figure 6*E* is aligned according to the crow's response, not by test onset (Fig. 6*F*). In this case, selectivity due to target position and target picture both reach maximal values just before the crow's response (time = 0 ms), with target position having a greater influence on neuronal activity than target picture. Trial outcome (i.e., correct or error) does not start to influence neuronal activity until after the response, when the crow receives feedback about trial outcome. Explained variance for factor "outcome" reaches a maximum after reward delivery. Note that this "outcome" activity difference between correct and error trials could reflect several sensory, motor, or reward factors related to the trial feedback, the expectation, delivery, and consumption of reward.

Discussion

We analyzed the response period of a DMS task, in which trained crows had to search for a previously remembered image in a choice array of 4 images. The crows performed the task

Table 2 Selectivity in other task periods

Percentage of cells selective for	All neurons ($N = 360$)	Position-selective neurons in the choice period ($N = 83$)	Picture-selective neurons in the choice period ($N = 55$)	Neurons selective for both factors in the choice period ($N = 28$)
Picture in the sample period	44% (159/360)	34% (28/83)	50% (27/55)	46% (13/28)
Picture in the delay period	18% (65/360)	24% (20/83)	22% (12/55)	36% (10/28)
Picture in both sample and delay periods	11% (38/360)	16% (13/83)	16% (9/55)	29% (8/28)
Trial outcome in the reward period	56% (204/358)	54% (45/83)	49% (27/55)	54% (15/28)

Note: Number of cells selective for different task-relevant factors in different task periods. Sample period: Kruskal–Wallis one-factor ANOVA in a 500-ms window starting 80 ms after sample onset. Delay period: Kruskal–Wallis one-factor ANOVA in an 800-ms window starting 200 ms after sample offset. Reward period: ranksum test in a 500-ms window starting 200 ms after reward delivery. Different neuronal subpopulations are selected based on selectivity in the choice period (Table 1).

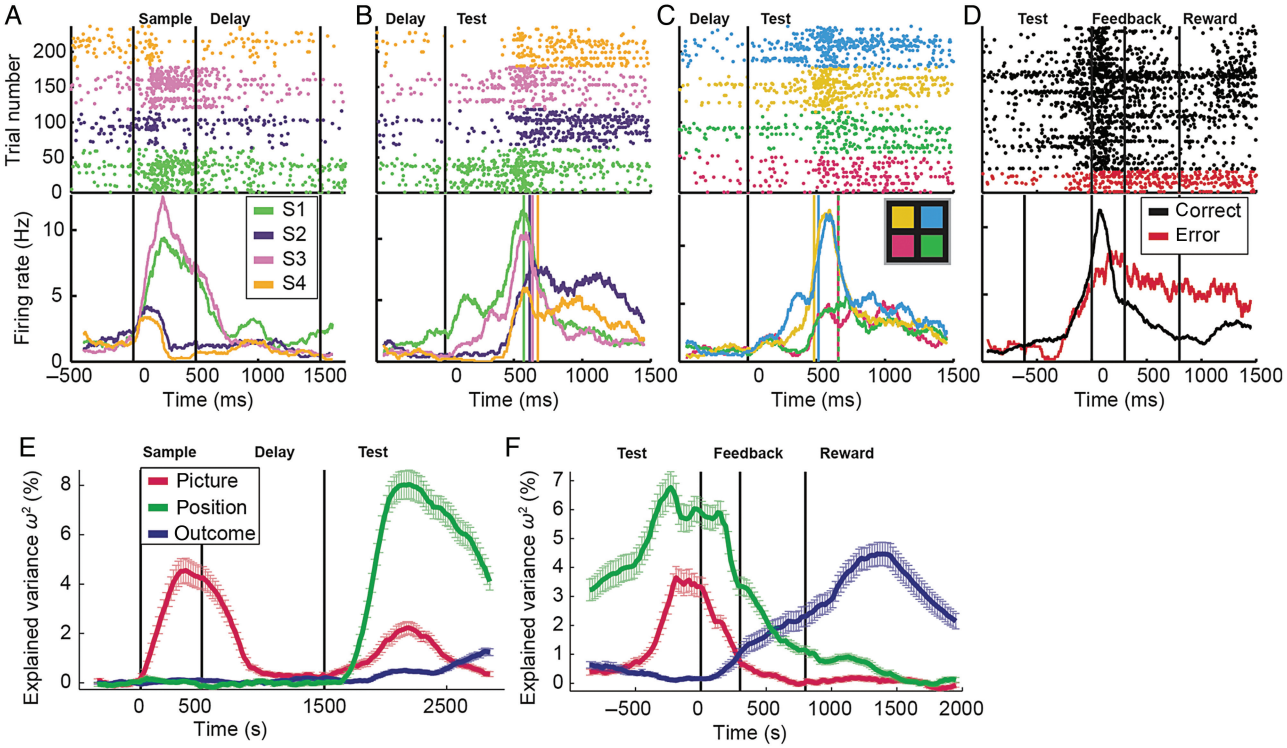

Figure 6. Comparison of spatial selectivity with selectivity to other task factors. (*A–D*) Example neuron which exhibits sample picture selectivity in the sample and delay period, selectivity for target position as well as picture during the choice period, and selectivity for trial outcome during the reward period. (*A*) Trials are aligned by sample onset; different colors represent different sample pictures. (*B*) Trials are aligned by test screen onset, and colors represent sample pictures. Colored vertical lines indicate median response times for each sample picture. (*C*) Trials are aligned by the test screen onset, and colors represent target positions. Colored vertical lines indicate median response times for each target position. (*D*) Trials are aligned by crow's choice. Vertical line marks median test screen onset. Colors represent trial outcome. (*E*) Percent explained variance (ω^2) derived from ANOVAs by sample picture, target position, and trial outcome during different task phases. Trials are aligned by sample onset. Error bars represent SEM across neurons ($N = 360$). (*F*) As in A, but trials aligned by crow's choice (time = 0 ms). Feedback about trial outcome is given at 0 ms, and reward is delivered at 700 ms (see Materials and Methods).

successfully, but exhibited patterns of performance and RTs consistent with serial visual search of the choice screen. Neurons in NCL, a multimodal association area in the avian brain, encoded the correct target position during the execution of the response. Compared with other behaviorally relevant variables in other task periods, encoding of target position had a particularly strong influence on neuronal activity in NCL. NCL neurons, both as a population and as single neurons, could dynamically change their tuning properties to represent behaviorally relevant task variables in different task periods.

Serial Visual Search

The behavioral performance and RTs of the crows, most prominently for crow K, are consistent with a serial scanning of all possible response positions until the target is found. The crows were not trained on this search strategy, and the position of the target was randomized and balanced across trials, so that the probability of a correct response and reward was equal for all 4 target positions. Nonetheless, the crows adopted behavioral strategies in the response period, which led to a bias of certain target positions over others. As we used highly complex visual images in our task, it is likely that the birds needed to adopt a strategy to scan all images serially. However, to test in more detail to which extent the crows were indeed using serial search, we would have to systematically increase the number of distractors and measure the influence on RTs. During pop-out search, the number of distractors has a minimal effect on RTs, whereas during serial search RTs increase linearly as a function of the number

of distractors in humans (Treisman and Gelade 1980; Wolfe and Horowitz 2004; Thornton and Gilden 2007), monkeys (Buschman and Miller 2009), and birds (Blough 1977).

The pattern of response times for different target locations seems similar to search patterns of rhesus monkeys performing a visual search task with 4 possible choices (Buschman and Miller 2009, 2010). The monkeys spontaneously adopted serial search patterns. This was evidenced by varying response times for different target positions during a visual search but not during a visual pop-out task. Even bees seem to employ serial search when forced to detect a colored disc among a varying number of distractor discs (Spaethe et al. 2006). Serial search thus seems to be an ubiquitous strategy across phylogenetic taxa.

This behavioral strategy in primates, bees, and crows represents a remarkable behavioral convergence in different groups of animals, which are separated by hundreds of millions of years of independent evolution. Similar convergence for visual information processing between birds and primates has been reported for barn owls and chickens. During free viewing, barn owls preferentially look at salient stimuli based on pop-out for stimulus orientation, and therefore show similar visual search characteristics for pop-out as primates (Harmening et al. 2011). Chickens can selectively direct visual attention to different areas of a screen based on visual cues (Sridharan et al. 2013, 2014), and thus show stimulus selection strategies parallel to primates in identical tasks (Moran and Desimone 1985; Carrasco 2011).

Encoding of Target Position

We report that single NCL neurons were tuned to different target positions during the visual choice period. During choice among 4 pictures in 4 corners of a touchscreen monitor, NCL neurons responded selectively based on the target position. NCL neurons in both hemispheres encoded spatial positions on the ipsi- and contralateral side of the screen, and the population formed a continuum with approximately equally strong preferences in the left/right or top/bottom directions, or combinations thereof, in individual neurons. These data suggest that ipsi- and contralateral space might be represented somewhat redundantly in the left and right NCL. Further studies are necessary to determine whether spatial representations in the 2 hemispheres are equivalent or whether they have different function and properties in the left and right NCL.

NCL activity in our study strongly correlated with target position, but our recordings cannot determine a causal relationship of spatially tuned NCL neurons with behavior. Lesion and inactivation studies of NCL, which can provide more causal evidence, have been performed in pigeons. These studies point toward a complex role of NCL in processing of motor behavior, with NCL inactivations leading to general behavioral inhibition in some studies (Helduser et al. 2013; Lengersdorf, Stüttgen, et al. 2014), but showing effects more specific to cognitive performance in others (Helduser and Güntürkün 2012). Recording studies in NCL of pigeons have reported correlates of premotor or sensorimotor behavior (Kalt et al. 1999; Starosta et al. 2013). Similar to our results in crow NCL, Lengersdorf, Pusch, et al. (2014) found NCL neurons which responded selectively depending on whether a pigeon would choose the left or right response key. These results implicate NCL in the selection and execution of responses. However, the task design used by Lengersdorf, Pusch, et al. (2014) could not dissociate response direction from perceptual decisions and sensory factors. We extend this work by investigating tuning of NCL neurons in 2D space, and controlling for any cognitive factors and response time variability, so that the reported selectivity clearly concerns the spatial location of the target. We similarly find a particularly strong representation of motor-related signals in NCL, with approximately 40% of NCL neurons discriminating between target positions.

Even with different behavioral controls, the spatial tuning of NCL neurons could additionally be influenced by several factors. Throughout the trial until the end of the delay period, the position of the crow's head was confined to a central position (as measured by a light barrier). During the following test period, the crow was free to peck. Thus, selectivity to different positions could correlate with movement of the head or eyes, and different visual or proprioceptive feedback. The choice period ended once the bird touched the screen to select a target. While the precise sensory or motor aspects that caused neuronal preferences for response directions need further exploration, these data suggest that NCL might be involved in directing and executing visually guided behavior. NCL therefore not only encodes a variety of cognitive aspects of behavior, such as the content of working memory (Veit et al. 2014; Moll and Nieder 2015; Veit et al. 2015), or abstract behavioral rules (Veit and Nieder 2013), but also participates in the translation of these cognitive processes to specific behaviors in the response period of the task.

Dynamic Tuning

In summary, our results show that NCL responds to visual stimuli, stores the behaviorally relevant stimulus information in working memory, and finally guides goal-directed behavior depending on that information (Fig. 6). NCL thus participates in all aspects of extended, goal-directed behavior, and represents sensory, cognitive, or motor factors required for successful execution of the given task. The population of NCL neurons dynamically adapted its neuronal representations to current demands over different task periods. Even individual neurons could dynamically change their tuning properties to encode the identity of visual images in the sample period, the position of the target image in the response period, and trial outcome in the reward period (Fig. 6A–D and Table 2). Single neurons could discriminate between sample images in the choice period, but not respond selectively to the same pictures during the sample period (Table 2). This pattern of selectivity argues that neuronal tuning to different parameters is not rigidly determined, but can rapidly change according to task demands, so that individual neurons can participate in the encoding of different parameters across different task periods.

This kind of selectivity is highly reminiscent of neuronal activity in primate prefrontal cortex (PFC), a proposed evolutionary analogue of NCL. PFC neurons encode visual working memory (Miller et al. 1996) and other cognitive factors during delayed response tasks (Miller and Cohen 2001). Moreover, neurons in the PFC can show directional selectivity based on the position of a target for goal-directed behavior (Goldman-Rakic 1995; Rao et al. 1997; Tanji et al. 2007; Kennerley and Wallis 2009; Funahashi 2013; Lennert and Martinez-Trujillo 2013) and motor actions (Asaad et al. 1998; Kobayashi et al. 2002). Importantly, PFC neurons dynamically adapt their tuning properties to different task demands, both as a population (Rainer et al. 1998; Stokes et al. 2013) as well as within single neurons (Rao et al. 1997; Kennerley and Wallis 2009; Funahashi 2013).

Our results suggest that NCL, an independently evolved brain area required for executive control of behavior in birds (Güntürkün 2005), exhibits similarly flexible coding properties and might represent one neuronal basis for corvid birds' exceptional cognitive abilities. These data add to the growing body of

evidence showing functional similarities between primate prefrontal neurons and corvid NCL neurons in comparable tasks, in a range of domains including quantity processing (Vallentin and Nieder 2008; Nieder 2013; Ditz and Nieder 2015), visual working memory (Fuster and Alexander 1971; Miller et al. 1996; Veit et al. 2014), abstract behavioral rules (Wallis et al. 2001; Veit and Nieder 2013; Ott et al. 2014), and learned associations (Fuster et al. 2000; Brincat and Miller 2015; Moll and Nieder 2015; Veit et al. 2015). So far, we have little evidence for functional differences between the 2 brain areas, with one notable exception concerning the time point when prospective representations emerge during association learning (Veit et al. 2015). The independent evolution of such a highly associative endbrain area in distantly related vertebrate groups argues that this flexible coding, with individual neurons tuned to various factors and capable of rapid recalibration depending on the demands of the current task, might be a key computational feature facilitating the emergence of complex cognitive behavior.

Authors' Contributions

L.V. and A.N. designed experiments, L.V., K.H., and A.N. performed experiments, L.V. analyzed data, and L.V. and A.N. wrote the paper.

Funding

This work was supported by a PhD fellowship from the German National Academic Foundation to L.V. and by the Deutsche Forschungsgemeinschaft (DFG) (NI 618/7-1) to A.N.

Notes

Conflict of Interest: None declared.

References

Asaad WF, Rainer G, Miller EK. 1998. Neural activity in the primate prefrontal cortex during associative learning. Neuron. 21:1399–1407.

Blough DS. 1977. Visual search in the pigeon: hunt and peck method. Science. 196:1013–1014.

Brincat SL, Miller EK. 2015. Frequency-specific hippocampal-prefrontal interactions during associative learning. Nat Neurosci. 18:576–581.

Buschman TJ, Miller EK. 2009. Serial, covert shifts of attention during visual search are reflected by the frontal eye fields and correlated with population oscillations. Neuron. 63:386–396.

Buschman TJ, Miller EK. 2010. Shifting the spotlight of attention: evidence for discrete computations in cognition. Front Hum Neurosci. 4:194.

Carrasco M. 2011. Visual attention: the past 25 years. Vision Res. 51:1484–1525.

Clayton NS, Dickinson A. 1998. Episodic-like memory during cache recovery by scrub jays. Nature. 395:272–274.

Clayton NS, Emery NJ. 2015. Avian models for human cognitive neuroscience: a proposal. Neuron. 86:1330–1342.

Ditz HM, Nieder A. 2015. Neurons selective to the number of visual items in the corvid songbird endbrain. Proc Natl Acad Sci USA. 112:7827–7832.

Durstewitz D, Kröner S, Güntürkün O. 1999. The dopaminergic innervation of the avian telencephalon. Prog Neurobiol. 59:161–195.

Emery NJ, Clayton NS. 2004. The mentality of crows: convergent evolution of intelligence in corvids and apes. Science. 306:1903–1907.

Funahashi S. 2013. Space representation in the prefrontal cortex. Prog Neurobiol. 103:131–155.

Fuster JM. 2008. The prefrontal cortex. 4th edn. San Diego: Academic Press.

Fuster JM, Alexander GE. 1971. Neuron activity related to short-term memory. Science. 173:652–654.

Fuster JM, Bodner M, Kroger JK. 2000. Cross-modal and cross-temporal association in neurons of frontal cortex. Nature. 405:347–351.

Goldman-Rakic PS. 1995. Cellular basis of working memory. Neuron. 14:477–485.

Güntürkün O. 2005. The avian "prefrontal cortex" and cognition. Curr Opin Neurobiol. 15:686–693.

Harmening WM, Orlowski J, Ben-Shahar O, Wagner H. 2011. Overt attention toward oriented objects in free-viewing barn owls. Proc Natl Acad Sci USA. 108:8461–8466.

Helduser S, Cheng S, Güntürkün O. 2013. Identification of two forebrain structures that mediate execution of memorized sequences in the pigeon. J Neurophysiol. 109:958–968.

Helduser S, Güntürkün O. 2012. Neural substrates for serial reaction time tasks in pigeons. Behav Brain Res. 230:132–143.

Hentschke H, Stüttgen MC. 2011. Computation of measures of effect size for neuroscience data sets. Eur J Neurosci. 34:1887–1894.

Hoffmann A, Rüttler V, Nieder A. 2011. Ontogeny of object permanence and object tracking in the carrion crow, *Corvus corone*. Anim Behav. 82:359–367.

Kalenscher T, Windmann S, Diekamp B, Rose J, Güntürkün O, Colombo M. 2005. Single units in the pigeon brain integrate reward amount and time-to-reward in an impulsive choice task. Curr Biol. 15:594–602.

Kalt T, Diekamp B, Güntürkün O. 1999. Single unit activity during a Go/NoGo task in the "prefrontal cortex" of pigeons. Brain Res. 839:263–278.

Karten HJ, Hodos W. 1967. A stereotaxic atlas of the brain of the pigeon: (Columba Livia). Baltimore: Johns Hopkins Press.

Kennerley SW, Wallis JD. 2009. Reward-dependent modulation of working memory in lateral prefrontal cortex. J Neurosci. 29:3259–3270.

Kobayashi S, Lauwereyns J, Koizumi M, Sakagami M, Hikosaka O. 2002. Influence of reward expectation on visuospatial processing in macaque lateral prefrontal cortex. J Neurophysiol. 87:1488–1498.

Kröner S, Güntürkün O. 1999. Afferent and efferent connections of the caudolateral neostriatum in the pigeon (*Columba livia*): a retro- and anterograde pathway tracing study. J Comp Neurol. 407:228–260.

Lengersdorf D, Pusch R, Güntürkün O, Stüttgen MC. 2014. Neurons in the pigeon nidopallium caudolaterale signal the selection and execution of perceptual decisions. Eur J Neurosci. 40:3316–3327.

Lengersdorf D, Stüttgen MC, Uengoer M, Güntürkün O. 2014. Transient inactivation of the pigeon hippocampus or the nidopallium caudolaterale during extinction learning impairs extinction retrieval in an appetitive conditioning paradigm. Behav Brain Res. 265:93–100.

Lennert T, Martinez-Trujillo JC. 2013. Prefrontal neurons of opposite spatial preference display distinct target selection dynamics. J Neurosci. 33:9520–9529.

Miller EK, Cohen JD. 2001. An integrative theory of prefrontal cortex function. Annu Rev Neurosci. 24:167–202.

Miller EK, Erickson CA, Desimone R. 1996. Neural mechanisms of visual working memory in prefrontal cortex of the macaque. J Neurosci. 16:5154–5167.

Moll FW, Nieder A. 2015. Cross-modal associative mnemonic signals in crow endbrain neurons. Curr Biol. 25:2196–2201.

Moll FW, Nieder A. 2014. The long and the short of it: Rule-based relative length discrimination in carrion crows, *Corvus corone*. Behav Process. 107:142–149.

Moran J, Desimone R. 1985. Selective attention gates visual processing in the extrastriate cortex. Science. 229:782–784.

Nieder A. 2013. Coding of abstract quantity by "number neurons" of the primate brain. J Comp Physiol A. 199:1–16.

Ott T, Jacob SN, Nieder A. 2014. Dopamine receptors differentially enhance rule coding in primate prefrontal cortex neurons. Neuron. 84:1317–1328.

Rainer G, Asaad WF, Miller EK. 1998. Selective representation of relevant information by neurons in the primate prefrontal cortex. Nature. 393:577–579.

Rao SC, Rainer G, Miller EK. 1997. Integration of what and where in the primate prefrontal cortex. Science. 276:821–824.

Spaethe J, Tautz J, Chittka L. 2006. Do honeybees detect colour targets using serial or parallel visual search? J Exp Biol. 209:987–993.

Sridharan D, Ramamurthy DL, Knudsen EI. 2013. Spatial probability dynamically modulates visual target detection in chickens. PLoS ONE. 8:e64136.

Sridharan D, Ramamurthy DL, Schwarz JS, Knudsen EI. 2014. Visuospatial selective attention in chickens. Proc Natl Acad Sci USA. 111:E2056–E2065.

Starosta S, Güntürkün O, Stüttgen MC. 2013. Stimulus-response-outcome coding in the pigeon nidopallium caudolaterale. PLoS ONE. 8:e57407.

Stokes MG, Kusunoki M, Sigala N, Nili H, Gaffan D, Duncan J. 2013. Dynamic coding for cognitive control in prefrontal cortex. Neuron. 78:364–375.

Tanji J, Shima K, Mushiake H. 2007. Concept-based behavioral planning and the lateral prefrontal cortex. Trends Cogn Sci. 11:528–534.

Taylor AH, Hunt GR, Medina FS, Gray RD. 2009. Do New Caledonian crows solve physical problems through causal reasoning? Proc R Soc B. 276:247–254.

Thornton TL, Gilden DL. 2007. Parallel and serial processes in visual search. Psychol Rev. 114:71–103.

Treisman AM, Gelade G. 1980. A feature-integration theory of attention. Cognitive Psychol. 12:97–136.

Vallentin D, Nieder A. 2008. Behavioral and prefrontal representation of spatial proportions in the monkey. Curr Biol. 18:1420–1425.

Vallentin D, Nieder A. 2010. Representations of visual proportions in the primate posterior parietal and prefrontal cortices. Eur J Neurosci. 32:1380–1387.

Veit L, Hartmann K, Nieder A. 2014. Neuronal correlates of visual working memory in the corvid endbrain. J Neurosci. 34:7778–7786.

Veit L, Nieder A. 2013. Abstract rule neurons in the endbrain support intelligent behaviour in corvid songbirds. Nat Commun. 4:2878.

Veit L, Pidpruzhnykova G, Nieder A. 2015. Associative learning rapidly establishes neuronal representations of upcoming behavioral choices in crows. Proc Natl Acad Sci USA. pii: 201509760. [Epub ahead of print].

Wallis JD, Anderson KC, Miller EK. 2001. Single neurons in prefrontal cortex encode abstract rules. Nature. 411:953–956.

Wolfe JM, Horowitz TS. 2004. What attributes guide the deployment of visual attention and how do they do it? Nat Rev Neursci. 5:495–501.

Wynne B, Güntürkün O. 1995. Dopaminergic innervation of the telencephalon of the pigeon (*Columba livia*): a study with antibodies against tyrosine hydroxylase and dopamine. J Comp Neurol. 357:446–464.